NIKHEF

NATIONAAL INSTITUUT VOOR KERNFYSICA EN HOGE-ENERGIEFYSIC

NIKHEF - K - AmPS 92-02 .

NIKHEF-K contributions to the 3rd European Particle Accelerator Conference, Berlin, march 24-28, 1992

AmPS, the Amsterdam Pulse Stretcher, as Photon Source
R. MAAS and G. LUIJCKX

Mechanical Design Philosophy and Construction of the Amsterdam Pulse Stretcher Ring AmPS
A.P. KAAN, J.H.M. BIJLEVELD, H. BOER ROOKHUIZEN, R.P.J. ARINK, J. TOUW, J.A. HEEMSKERK

80 kV Electrostatic Wire Septum for AmPS
A. VAN DER LINDEN, J.H.M. BIJLEVELD, H. BOER ROOKHUIZEN, P.J.T. BRUINSMA, E. HEINE, P.LASSING, E. PRINS

Pulsed Electrostatic Kickers with Low Beam Impedance for AmPS
E. HEINE, A. VAN DER LINDEN, J.H.M. BIJLEVELD, P.J.T. BRUINSMA, J.J. KUIJT, P.F. TIMMER

High Power Density, Thin Magnetic D.C. Septa for AmPS
A. VAN DER LINDEN, J.H.M. BIJLEVELD, H. BOER ROOKHUIZEN, P.J.T. BRUINSMA, M. DOETS, P. LASSING, C. ZEGERS

Improvement of the 400 kV linac electron source of AmPS
F.B. KROES, M.G. VAN BEUZEKOM, N.J. DOBBE, J.T. VAN ES, P.P.M. JANSWEIJER, A.H. KRUIJER, G. LUIGJES, T.G.B. SLUIJK

NIKHEF SECTIE - K POSTBUS 4395, 1009 AJ AMSTERDA

The Amsterdam Pulse Stretcher AmPS as a Photon Source

R. MAAS and G. LUIJCKX
National Institute for Nuclear and High Energy Physics (NIKHEF),
P.O. Box 41882, 1009 DB Amsterdam, the Netherlands

Abstract

AmPS, an electron Pulse Stretcher/Storage Ring will start delivering nearly continuous electron beams of maximum 900 MeV in Spring 1992. The extracted beam (using the machine in Stretcher Mode) as well as the stored beam (in conjunction with an internal gas-jet target) will be used for nuclear physics purposes for about 2500 hours/year. For the remaining time of the year AmPS could be used as a dedicated Photon Source covering the spectrum from infrared up to soft X-rays. The synchrotron radiation properties of the actual machine are presented together with a design for a modified ring lattice. The modification only requires the addition of focussing elements to the actual machine so the characteristics in "nuclear physics" mode are not affected. The new lattice will allow AmPS to be operated in a low-emittance mode (ε = 4.5 x 10^{-9} rad.m @ 900 MeV) providing a SR brilliance from its bending magnets of 2 x 10^{14} photons / s / mrad^2 / mm^2 / 100 mA / 0.1 % BW. Further enhancement of the brilliance can be achieved by the implementation of multipole undulators. The ring can accommodate such insertion devices in one of its 32 m long straights.

1. INTRODUCTION

AmPS operating in Storage Mode will store currents up to 200 mA. The AmPS ring has a "square" shape with a fourfold symmetric structure. Each quadrant comprises an achromatic curve (l = 20.8 m) with straights (l = 16.1 m) on either side; circumference is 212 m. The magnet lattice is of the FODO type and consists of 32 dipoles, 68 quadrupoles and 32 sextupoles. The project has been described in full detail in [1].

2. SYNCHROTRON RADIATION FROM THE PRESENT LATTICE

General: synchrotron radiation will be available from the 32 dipoles (ρ = 3.3 m) of AmPS. The ring has 4 straight sections of which two sections can accommodate insertion devices. Table 1 shows general SR parameters of AmPS.

Spectrum: the AmPS ring has been designed to operate from 300 MeV to 1.0 GeV. The characteristic energy of the SR from the bending magnets can therefore be shifted from 20 eV at 300 MeV to 665 eV at 1 GeV. A superconducting wavelength shifter with a strength of 8 T can extend the characteristic energy to about 5 keV.

Photon flux and brilliance: the photon flux from the dipoles is comparable with the flux from other SR sources.The present usage of AmPS (Stretcher + Internal Target Physics) doesn't require low emittances and small beam sizes. The SR brilliance of the source therefore is presently not competitive with the new generation of machines.

3. LOW EMITTANCE LATTICE

3.1. Basic concept

The transverse emittance ε_x can be expressed as

$$\varepsilon_x = C_q \gamma^2 \frac{I_5}{I_2 - I_4} \qquad (1)$$

C_q is a lattice-independant constant; I_n are the synchrotron integrals. $I_2 = 2\pi/\rho$; for a given set of dipoles, therefore, I_2 is a constant. For rectangular dipoles, see ref [2], $I_4/I_2 \approx -\pi^2/(3N_d^2) = -3.2\times10^{-3}$ (N_d is number of dipoles).

Table 1. General SR characteristics of the actual AmPS ring

SR from ring dipoles				
electron energy	[GeV]	0.3	0.6	0.9
circulating current	[A]	0.2	0.2	0.2
dipole field	[T]	0.3	0.6	0.9
characteristic energy (ε_c)	[keV]	0.02	0.14	0.49
energy loss/turn	[keV]	0.22	3.5	17.4
photon flux	[10^{12} *]	0.48	0.96	1.44

* photons/s/mrad/100 mA/0.1 % BW

A decrease of the value of ε_x, therefore, implies decreasing the value of I_5. The value of I_5 strongly depends on the dispersion function inside the dipoles: in all low-emittance lattices the dispersion function inside the dipoles is small.

3.2. *Possible low-emittance structures*

Since we are dealing here with an adaption of an existing lattice, with the additional condition of retaining the functionality of the present lattice, the possibilities of modification are somewhat restricted.
Basically four structures have been considered:

- double focussing achromat (DFA): FD–[B]–F–[B]–DF
- triple achromat (TA): [B]–FDF–[B]
- triple bend achromat (TBA): FD–[B]–F–[B]–F–[B]–DF
- FODO structure F–[B]–D–[B]

F and D indicate focusing and defocusing quads respectively; B is a dipole. The minimum emittance obtainable with these structures can be expressed as

$$(\varepsilon_x)_{min} = C_q \gamma^2 \theta^3 f \qquad (2)$$

θ is the dipole bending angle (rad) and f is a structure-dependant factor (e.g. f(DFA) = 6.45×10^{-2}; f(TBA) = 5.02×10^{-2}). Comparing $\theta^3 f$ with the present value of I_5/I_2 indicates that theoretically the emittance can be reduced by a factor 350–250.

FODO structure

Each of the four cells comprising a Curve is basically a FODO cell; since such a cell contains two dipoles, the structure is **not** dispersion-free. In order to match the FODO cells to the dispersion-free straights, a *dispersion suppressor* is needed. The following structure, (Fig. 1), containing 4 dipoles, is composed from two regular (Curve) cells, and comprises one FODO cell + dispersion suppressor:

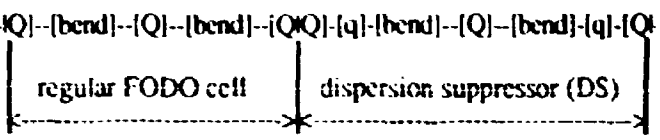

Fig. 1 Half a Curve; the structure of a full Curve is (DS)–(FODO)–(FODO)–(DS). The physical lengths of (FODO) and (DS) are equal. Four additional quads/Curve ([q]) are needed.

Since the dispersion function in a FODO cell is never ve low (here it oscillates between 0.35 and 0.90 *m*), t equilibrium emittance will also not be very low:
ε_x (@900 MeV) = 32×10^{-9} rad. m.
(i.e. reduction by factor 5 w.r.t. present lattice)
$\chi_x = -8.1$ $\chi_y = -14.8$
This relatively small reduction factor of the emittance mal this structure for our machine not very interesting.

TBA's

Each Curve comprises 8 dipoles (4 cells); 1 $\frac{1}{2}$ cell (containi 3 dipoles) can be converted into a triple bend achromat (TB/ Two additional quads per TBA are needed. Using 6 out o total of 8 dipoles (i.e. 3 cells) yields two TBA's. T remaining cell (containing two dipoles) should be used 'connect' the two TBA's. Constructing the TBA's is not t problem; the problem is to construct from the one remaini cell (and within the space occupied by that cell) (achromatic) match between the two TBA's:

[TBA]—[achr. match of 2 dipoles]—[TBA]

This problem has not been solved yet. Another possibility to connect the two TBA's directly, and put one dipole on eit end of the structure:

[one dipole-match]—[TBA]—[TBA]—[one dipole-match

Table 2. SR source parameters at 0.9 GeV; present lattice and improved lattice ('mod(a)').

		lattice type	
		present	improved
horiz. beam emittance (ε_x)	[10^{-9} rad.m]	160	4.8
horiz. beam size (σ_x) in dipole	[μm]	690	85
vert. beam size (σ_y) in dipole	[μm]	87	21
natural SR vert. divergence at ε_c	[μrad]	290	290
brilliance	[10^{12} **]	5.7	190

** photons/s/mrad^2/mm^2/100 mA/0.1 % BW

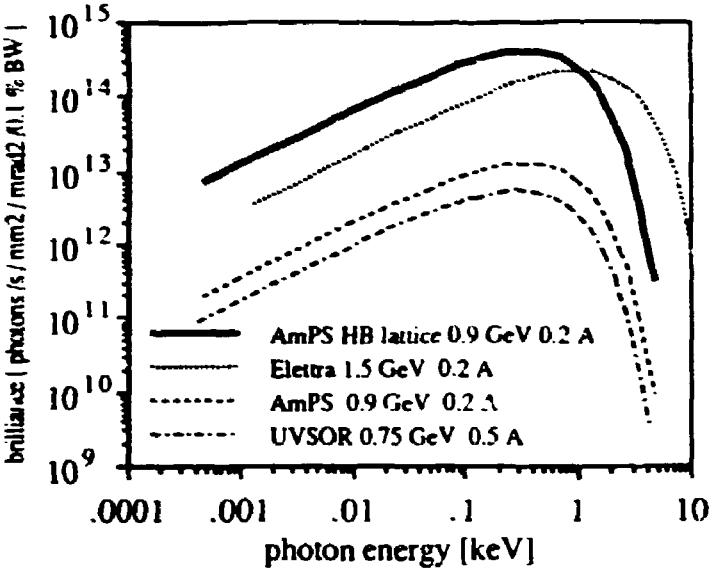

Fig.2 AmPS brilliance (present and modified lattice) compared to Elettra and UVSOR brilliance.

This match is not achromatic; therefore the TBA should already start with non-zero dispersion, thus increasing the dispersion function in *all* the TBA magnets: the structure will acquire FODO-like properties. This is probably not a fruitful approach.

3.3. AmPS lattice modification

Each of the 4 curves of AmPS comprises 4 cells of the following configuration:

F—[B]—D—[B]—F

Adding a quad either on the inside or outside of each dipole (and changing the polarity of the central quad) will result in a DFA-like structure, see Fig. 3:

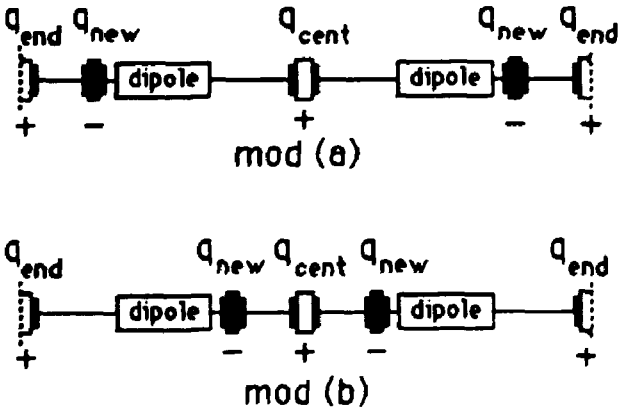

Fig. 3 Modification of cell structure (solid :added quadrupoles); each of the 4 Curves comprises 4 of these cells.

Each Curve contains two families of sextupoles (2 per cell) to control the chromaticity; these sextupoles are not shown in Fig. 3. In Table 3 some properties of the two configurations have been summarized. Configuration 'mod(b)' clearly reduces the emittance the most; however, this structure introduces much more chromatic aberrations than configuration 'mod(a)'. Before a final decision will be made about the modification configuration, a more thorough analysis will be made about chromaticity control, dynamic aperture and sensitivity of the modified lattice.

Table 3. Quadrupole tipfields (E = 0.9 GeV) and emittance-related data of configurations mod(a) and mod(b), see Fig. 1. Dimensions of q_{new}: l = 0.105 m; ϕ = 71 mm

		mod(a)	mod(b)
$B_{tip}(q_{end})$	[kG]	7.87	8.08
$B_{tip}(q_{cent})$	[kG]	8.28	9.60
$B_{tip}(q_{new})$	[kG]	-8.73	-8.95
ε_x(0.9 GeV)	[rad.m]	4.8×10^{-9}	1.1×10^{-9}
χ_x		-18.0	-63.0
χ_y		-13.9	-34.1
$\varepsilon_{present}/\varepsilon_x$		33	149
I_5 / I_2		4.06×10^{-3}	0.91×10^{-3}

4. PROPERTIES IMPROVED LATTICE

The resulting SR brilliances from dipole radiation for the actual and the improved lattice ('mod(a)', Fig.3) are shown in Fig. 2. The graph clearly shows the competitive position of AmPS with respect to some of the new generation machines. In Table 2 important source parameters are summarized.
A possible set-up for SR beamlines including insertion devices has been presented in [3].

5. CONCLUSIONS

It is possible to adapt the AmPS lattice to operate either in a high or a low emittance mode. In the low emittance mode the AmPS ring will provide a competitive photon flux and a high brilliance when compared to other synchrotron radiation sources.
The ring will operate for nuclear physics experiments during 2500 hours/year. Therefore dedicated use of the ring for SR experiments would be feasible up to about 2000 hours/year provided funding is available.

6. REFERENCES

[1] G. Luijckx e.a., "Status of the Amsterdam Pulse Stretcher Project " Proc. 2nd European Accelerator Conference (EPAC 1990), pp. 589-591.
[2] J.A.Uythoven, J.I.M. Botman and H.L. Hagedoorn, "Analytical evaluation of synchrotron radiation integrals for isomagnetic lattices with rectangular dipole magnets". Proceedings EPAC (Rome, June 7-11, 1988), p.649
[3] Guy Luijckx and Rob Maas, "Synchrotron Radiation from the Amsterdam Pulse Stretcher (AmPS)" Proc. 4th International Conference on Synchrotron Radiation Instrumentation [SRI-1991], Review of Scientific Instruments, Vol.63, No.1 (part II B) pp.1621-1622.

Mechanical Design Philosophy and Construction of the Amsterdam Pulse Stretcher Ring AmPS

A.P. Kaan, J.A. Heemskerk, J. Touw, J. Bijleveld, H. Boer Rookhuizen,
W. Verlegh, J. Langedijk, G. Bron, R. Arink, P. Lassing
National Institute for Nuclear Physics and High-Energy Physics (NIKHEF-K)
P.O. Box 41882
1009 DB Amsterdam, The Netherlands

Abstract

The AmPS ring is a 900 MeV electron pulse stretcher and storage ring with a circumference of 212 m. The ring will be completed early 1992. Apart from the UHV envelope for the beam the ring contains a large quantity of high precision components, e.g. 166 magnetic elements, 50 beam monitors, an r.f. cavity, 2 injection kickers, etc. An overview is presented of the design philosophy and the construction with emphasis on the vacuum components as well as on the alignment system and on the supports for the magnets and the monitors. The material of the vacuum components has been chosen on the basis of the requirement that outgassing, synchrotron radiation induced desorption, residual radioactivity and magnetic permeability should be as low as possible. The vacuum chambers in the bending sections therefore are fabricated from stainless steel 316 LN with a very low cobalt content. An advanced welding and cleaning technique has been developed to avoid the inclusion of impurities. The vacuum pump capacity and the pump distribution along the ring has been optimised as function of local conductances and outgassing. With eighty 60 l/s ion pumps a net pump capacity of 20 l/s/m should be obtained.

Vacuum aspects

The specifications of the vacuum system were presented in [1]. The determining factor for the vacuum pressure is the quantum lifetime of one hour for a stored beam at the lowest operational energy of 300 MeV yielding a pressure of < 1×10^{-8} mbar.
The vacuum pressure should be achieved with lumped Starr cell iongetter pumps only. It was calculated that a total pumping speed of 4320 l/s is required.
With respect to the article [1] the construction of the vacuum chamber and the positioning of the pumps has been changed. The overall advantage of using an antechamber to trap the gas desorption caused by the synchrotron radiation appeared to be rather small because of the slot structure required at the exit port.

Two mobile units each with a turbomolecular drag-pump as main pump and a membrane pump will be used as an oil-free roughing pump. The ring consists of 5 separate vacuum sections. Each section can be isolated by rf compatible straight through valves (VAT). All metal angle valves allow to connect the turbo pumps to the ring. A lifting mechanism brings the pump unit in position after which the unit is coupled directly to the ring without using a bellows connection. A quadrupole mass spectrometer (Balzers QMA 125) is integrated in the unit to leak chase or analyse vacuum problems.

Prior to assembly all parts are chemically cleaned. The assembled parts are then baked for 24 hours at about 250° C in a vacuum oven. Venting with dry nitrogen provides a good surface condition for the vacuum parts before installation. At this moment, March 1992, three of the four 22 m long curves of the ring have been evacuated and are at a pressure of 2×10^{-9} mbar.
Conflat type seals are used where ever possible because of the reliability.

Mechanical aspects

Vacuum chamber configuration

Optical studies [2] and safety margins for closed orbit errors determined the beam stay clear dimensions of the vacuum enclosures. The feasibility of the fabrication was then to be optimised within the budget constraints. In the curved sections the beam stay clear in the vertical direction is 32 mm and 65 mm in the horizontal direction.

Space for ion clearing electrodes increased the vertical inner dimension of the enclosures to 40 mm. The vacuum wall thickness could be reduced to 2 mm because stainless steel 316 LN [1] has been chosen instead of aluminium. Including a 1 mm clearance between the chamber and the magnet poles the magnet gap became 45 mm (fig. 1).

In the straight sections the quadrupole magnets have a bore of 95 mm. So circular pipe of 94 mm was suitable, except for the extraction and the injection region where additional space is required because of large beam excursions at these locations. The injection and extraction septa are described in [3].

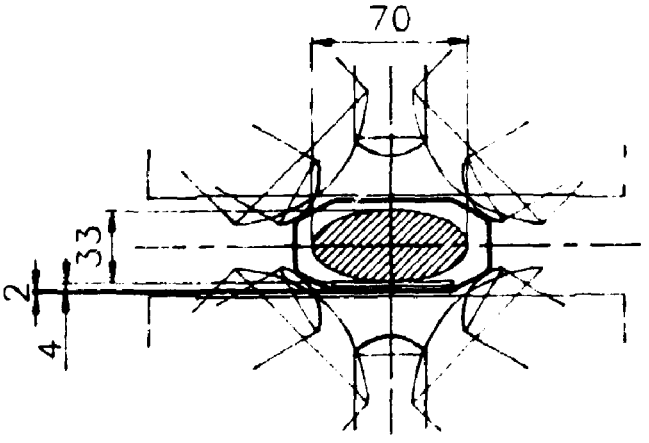

Fig. 1 The boundary conditions for the vacuum chambers

Alignment

The alignment accuracy of the magnetic elements of the ring were determined by beam optical calculations. These studies resulted in a positioning accuracy requirement of 0.1 mm for the quadrupole and sextupole magnets and 0.5 mm for the dipole magnets.

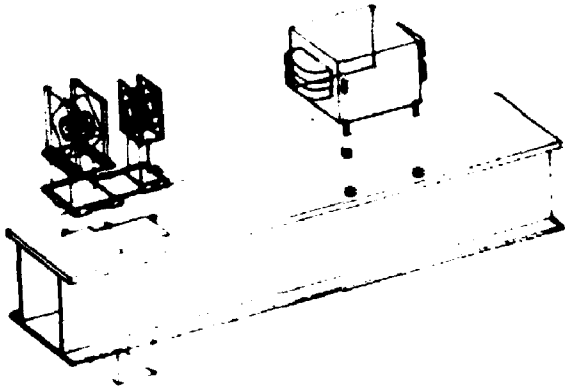

Fig. 2 Positioning and adjustment supports optical elements

All beamline components are aligned (fig. 2) and mounted on so called strongbacks. For the curved sections 16 strongbacks are use, each consisting of a heavy and rigid steel construction weighting 6 tons. The surface of these supports are milled within a tolerance of 0.1 mm. Numerical machined holes in the supports are positioned with an accuracy of < 0.1 mm. The bending magnets are supported and adjusted in height by three bolts. These bolts fit in accurately positioned holes in the magnet. The other components are pre-aligned on x y z tables. By means of a laser alignment system the beamcentre line is translated to an external reference line 50 cm above the beamline. This way the cells are aligned as one unit in the reference line in the tunnel (fig. 3).

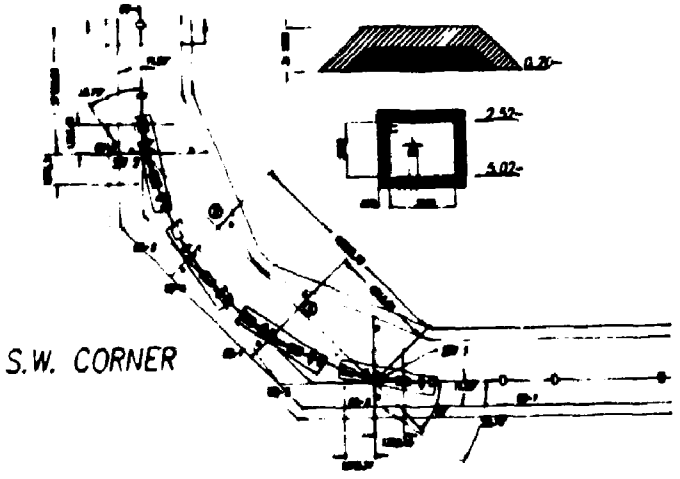

Fig. 3 Reference lines in the curved sections

A spare strongback fitted with exactly the same holes and reference points is available to allow easy reinstallation of repaired or modified components.

Manufacturing

Vacuumchambers

To minimise the costs the beam pipe in the curved sections is made by folding stainless steel sheet with a thickness of 2 mm. 316 LN material was chosen to obtain a low permeability remaining stable after machining and welding. The influence of welding on the magnetic properties of the material was compared for 304L, 316L and 316 LN by measuring the μ with a magnetic permeability meter (Dr. Förster Institut). The material 316 LN appeared to be much more stable with respect to this property. Depending on the intensity of welding the μ went to 1.1 or even 1.2 for the first two types of stainless steel. Baking the material to about 400° C almost did recover the 1.01 starting position. The increase of μ_r was much lower for the 316 LN (< 1.01). After annealing the value became 1.004.

Fig. 4 The different stages in folding the vacuum pipe

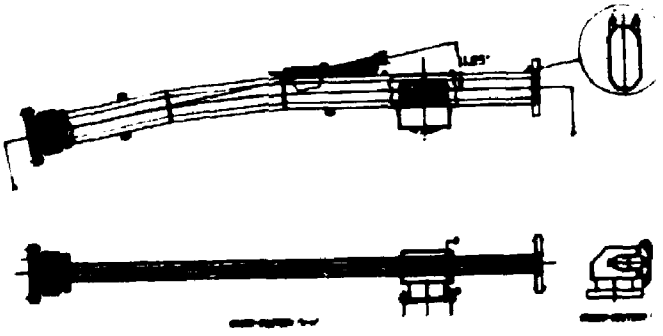

Fig. 5 The segmented vacuum chamber with integrated pump out

The way the vacuumchambers are folded requires only one closing weld (fig. 4). Argon arc welding was performed on a lathe semi automatically for the long seems while handwelding was used for the short welds. Backing with argon gas was done consequently in order to prevent oxidation on the inner surface. Inner welding was performed where possible. When there was no other way a completely through weld was applied to avoid gas enclosures in the vacuum system.

The curve in the dipole magnets was approximated by three straight parts which are welded together (fig. 5). Each curve contains 8 dipole vessels. In total 5 dipole vessels have a synchrotron light port for monitoring purposes. The heat load generated by the synchrotron radiation (3.5 kW at 900 MeV and 200 mA in total for the whole ring) can be handled without cooling. Nevertheless at the points where the radiation is extracted the mechanical tension could be high. Therefore a water cooled copper bloc has been soldered on the stainless steel wall.
In the straight sections 316L stainless steel is used because no permeability deteriorating welds were required in the direct vicinity of the magnets. The Conflat sealing flanges are welded to the beampipes. As no field welds were made because for cleanliness reasons all magnets can be splitted in halves to allow the installation of the vacuum pipes.

The stripline type position monitors appeared to be very sensitive for higher order rf modes generated by the beam. Therefore rf damping of these modes has been incorporated [illegible] aluminium oxide pipes coated with resistive paint [4]. The desorption properties of this material were measured [5] and compared to the desorption of an alternative absorber consisting of ferrite. Roughly the ferrite desorption is 10 times higher than the Al_2O_3 desorption. After 1 week of outgassing a desorption of $1x10^{-9}$ mbar l/s/cm^2 was measured for the Al_2O_3.

The clearing electrodes are made as smooth as possible and consist of a button of Ø 40 mm 2 mm above the bottom of the vacuum chamber (fig. 6).

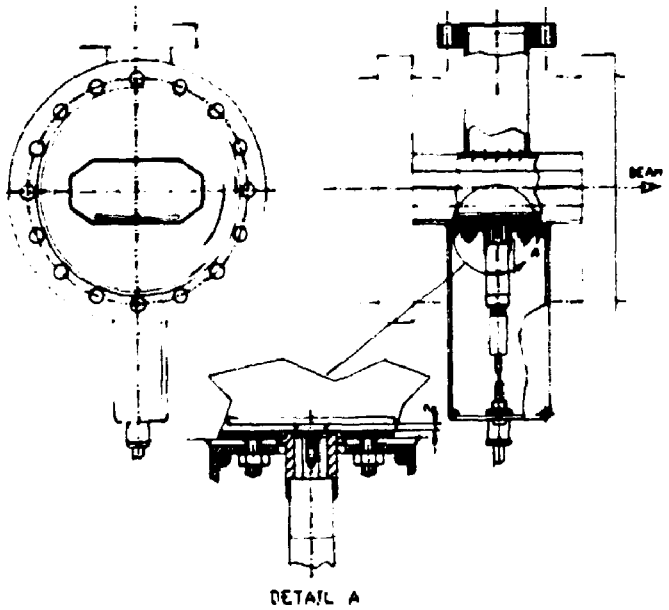

Fig. 6 Clearing electrode

The pump out design was optimised for maximum vacuum conductance and low rf impedance. At the locations where pumps are connected the vacuum pipe is perforated and a housing is build around that location such that the total conductance is twice as large as the conductance of the connecting pipe to the pump.

In order to bridge the slits in the Conflat flange joints a special spring contact shielding was developed that is mounted together with the sealing ring (fig. 7).
An rf shielding sleeve is fitted in each beampipe bellows. The sleeves were manufactured by photo-chemical etching.

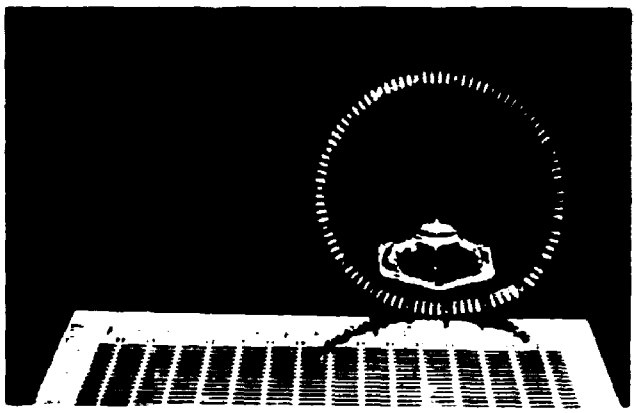

Fig. 7 Rf shielding Conflat flange

Acknowledgment

This work is part of the research programme of the National Institute for Nuclear Physics and High-Energy Physics (NIKHEF), made possible by financial support from the Foundation for Fundamental Research on Matter (FOM) and the Dtuch Organization for Scientific Research (NWO).

References

1) A.P. Kaan e.a. Vacuum/vol. 41/numbers 7-9, 1890
2) R. Maas e.a., Internal Nikhef report: AmPS 88-11
3) A. v/d Linden e.a., This conference.
4) D. Moffat et al., "Use of Ferrite-50 to Strongly Damp Higher Order Modes" Proc. IEEE Particle Accelerator Conf. San Francisco, CA, May 1991
5) Internal NIKHEF report 'Outgassing of damping material'

7/8

80 kV Electrostatic Wire Septum for AmPS

A. van der LINDEN, J.H.M. BIJLEVELD, H. BOER ROOKHUIZEN, P.J.T. BRUINSMA, E. HEINE, P. LASSING, E. PRINS
National Institute for Nuclear and High Energy Physics (NIKHEF),
P.O. Box 41882, 1009 DB Amsterdam, the Netherlands

Abstract

In the extraction process of the Amsterdam Pulse Stretcher (AmPS) the extracted beam is intercepted from the circulating beam by the 1 m long electrostatic wire septum. For a bending angle of 4.4 mrad the maximum anode voltage is 80 kV.

An innovative mechanical construction has been developed to create a wire spacing of 0.65 mm between tungsten wires of 50 µm diameter. Stainless steel spring wires, bent on a half-cylindrical carrier, stretch the septum wires two by two. This insures that eventually broken wires are retracted.

Care has been given to the electric field distribution at the entrance and exit of the septum and to the insulators, required to support the anode. Prototype tests have been successful up to an anode voltage of 120 kV.

1. INTRODUCTION

The AmPS ring aims at a 100 % duty cycle operation by means of slow extraction of injected electron beam pulses of 2.1 µs, as described by Luijckx et.al. [1]. The maximum beam energy is 900 MeV. The minimum time for extraction is 2.5 ms and the maximum extracted d.c. current is 67 µA. AmPS can optionally be used as a storage ring with an internal target.

The third integer resonance of the horizontal betatron oscillation is excited to give the circulating beam large horizontal excursions. The electrostatic extraction septum intercepts and separates the extracted beam from the circulating beam. The extracted beam is directed outwards horizontally between the massive anode and the grounded, thin cathode of the electrostatic septum. The cathode, called the septum, acts as knife for the interception of extracted beam and screens the electrostatic field for the circulating beam. The separation between the extracted and circulating beam is enlarged by the next two ring quadrupole magnets, as shown in Figure 1. Finally, the extracted beam is bent outwards horizontally by the magnetic extraction septum [2] and is sent along the AmPS extraction line.

2. OPTICAL REQUIREMENTS

Maas [3] has simulated the extraction process. The pitch of the extracted beam, being its horizontal width, is calculated to be of the order of 8 mm for a horizontal septum location of 30 mm, with respect to the ring axis. The gap width between the anode and the cathode is required to be 20 mm. The position and direction of the septum must be adjustable.

The allowed beam loss, due to interaction with the septum, is about 1 %. This restricts the effective septum thickness to 100 µm. The septum thickness is chosen to be 50 µm.

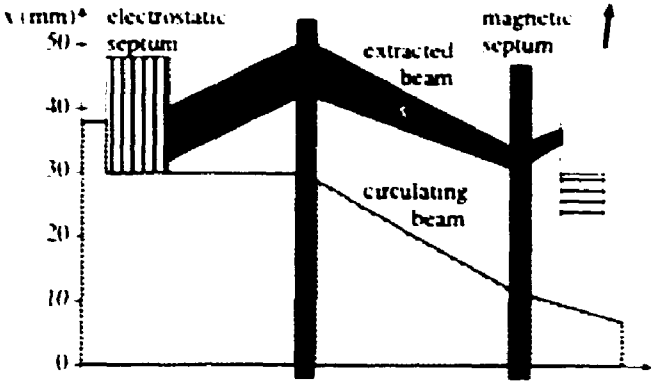

Figure 1 - Schematic layout of the AmPS beam extraction.

Hoekstra [4] has required that the extracted beam arrives at a horizontal position of 220 mm with respect to the ring axis. As a result of optimization, the electrostatic extraction septum is required to be 1 m long and to have a bending angle of 4.4 mrad. This determines the maximum electric field strength to be 40 kV/cm, requiring a maximum anode voltage of 80 kV.

3. WIRE SEPTUM REQUIREMENTS

3.1. Design principles

Based on qualitative grounds, the design of a wire septum is considered. Mechanically, nearly one-dimensional forces can be applied to wires in order to create a flat, thin septum plane, consisting of an array of wires. Concerning the heating of the septum due to the interaction with beam particles, wires have the optimal ratio of radiant surface and heated volume.

3.2. Septum heating requirements

The interaction of the electron beam with the wire material is characterized by the heat production due to the beam energy loss. The maximum current, interacting with a 50 µm thick wire, is calculated as 0.42 µA. According to Koechlin [5], the maximum temperature of a tungsten septum wire is 1600 °C for a beam height of 1.6 mm, assuming cooling by radiation only. However, the tensile strength of 2 kN/mm^2 starts to decrease at 1200 °C due to recrystallization processes.

3.3. Electric field strength requirements

Considering the septum wires as the field emitting cathode, the electric field strength at the wire surface is determined by the conservation of the flux of electric field lines:

$$E_0 \cdot a = E_w \cdot \pi \cdot t \qquad (1)$$

where E_w is the field strength at the wire surface and E_0 is the

average electric field strength between anode and cathode, a is the wire spacing and t is the wire diameter.

Dubois and Garrel [6] have determined experimentally the maximum average field strength for a tungsten wire septum. According to (1), the maximum field strength at the tungsten wire surface is calculated as 167 kV/cm. The wire spacing for the AmPS electrostatic septum is then restricted to 0.65 mm, according to (1). These results have been confirmed by the theory of planar triodes, described by Kleijnen and Jonker [7].

According to Durand et.al. [8], a wire spacing of 0.65 mm results in an effective average field strength of 39.7 kV/cm at the maximum anode voltage of 80 kV. The field strength, experienced by the circulating beam, is 78 V/cm, which makes the transparency of the septum 0.2%.

If all wires have the maximum temperature of 1600 °C, the field emission of the 1 m long septum is 0.82 mA in worst case. The high voltage power supply requirements are met by the 100 kV/1.5 mA supply of the Gamma RR series.

3.4. Mechanical requirements

To prevent a high voltage short-circuit in case of a broken wire, the construction of the plane array of thin wires requires a springloading force. This has been approached by an innovative technique of spotwelding septum wires to cylindrically curved spring wires. The spring wires are curved along half a cylinder, called the carrier. The bending moment of one spring wire is used to stretch two septum wires. The two ends of a piece of septum wire are spotwelded at the same parallel end of a spring wire. Then the septum wire is looped around the other end of the spring wire. Figure 2 shows the principle design.

The spring wires of 0.6 mm diameter are placed in grooves with a spacing of 1.3 mm. The septum wires are positioned by precision machined grooves in the two ridges of the carrier. Due to electrostatic forces acting upon the septum wires, the high voltage electrode is located inside the carrier construction.

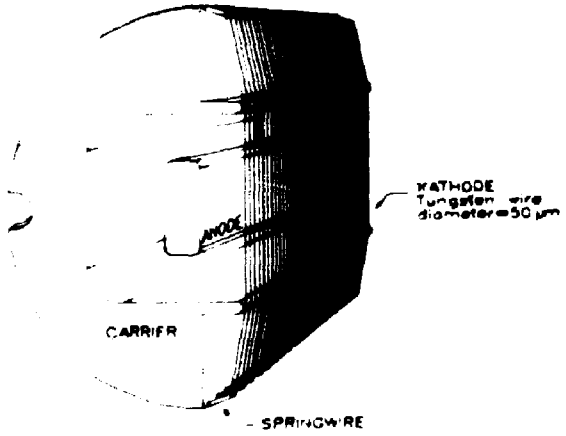

Figure 2 - A 3-D view of the principle wire septum design.

To restrict the electrostatic repulsion of adjacent wires, the minimum stretching force is determined by the proportional chamber wire instability. According to Anderson et.al. [9], using Durand et.al. [8], the minimum force is 0.09 N for a 80 mm long wire. The resulting minimum stress is 45 N/mm^2.

Taking into account the decrease of the tensile strength of tungsten at high temperatures the septum wire stress is optimized as 200 N/mm^2. This results in a required stretching force of 0.4 N. The length of the parallel ends of a spring wire and its radius of curvature are optimized as 19 mm and 86 mm respectively. Regarding the tensile strength of stainless steel spring wires of 1000 N/mm^2, the resulting maximum stress in a spring wire is 720 N/mm^2.

4. HIGH VOLTAGE REQUIREMENTS

4.1. High voltage electrode dimensions and location

In order to obtain a stiff carrier construction the high voltage electrode has been optimized with regard to the electric field strengths. As shown in Figure 2, the cross-sectional area within the carrier is restricted to be 70 mm wide and 80 mm high. The cross-section of the electrode is optimized as 20 mm thick and 40 mm high with rounded corners of 7.5 mm radius. At the maximum anode voltage of 80 kV the maximum field strength has been calculated to be less than 75 kV/cm near the corners opposite to the plane of wires.

To obtain a uniform electric field distribution at the exit and entrance of the septum, field clamps are added to the symmetric anode design. As a result of Poisson calculations, the anode is bent backwards by 30°, as shown in Figure 3. At the septum exit the anode is folded back around the carrier to be connected to the centred high voltage vacuumfeedthrough.

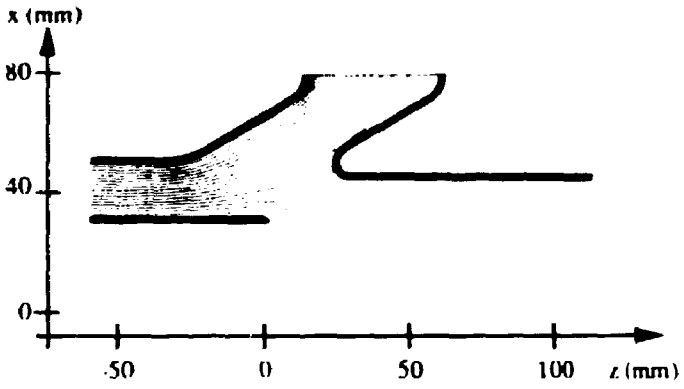

Figure 3 - Poisson plot of equipotential lines for the design of the field clamps and anode at the septum entrance and exit.

4.2. High voltage insulator design

For mechanical reasons, the high voltage electrode has to be supported by the grounded carrier at 3 places along its 1 m length. From prototype tests, the 30 mm wide area in between the backside of the anode and the grounded carrier is found too narrow for an aluminumoxide insulator to hold off the required 80 kV long enough for operational use. This is explained by breakdown in splits between carrier and insulator and by flash over along the insulator, due to upbuilding of positive charge by secondary electron emission.

The final insulator design consists of a deep pit in the carrier and a shallow pit in the anode to decrease the field strength near the metal surfaces. The insulator is a 57.5 mm long rod of aluminumoxide of 10 mm diameter. The rod ends are metallized and provided with metal screw-threads at both ends to prevent breakdown in splits.

As shown in Figure 4, Poisson calculations have proven that the field strength in the area of the insulator is lower than elsewhere between anode and cathode. Therefore it is expected that breakdown and flashover processes are less likely to occur and that the insulator area is also screened from the free charge particles, which are possibly present during ring operation.

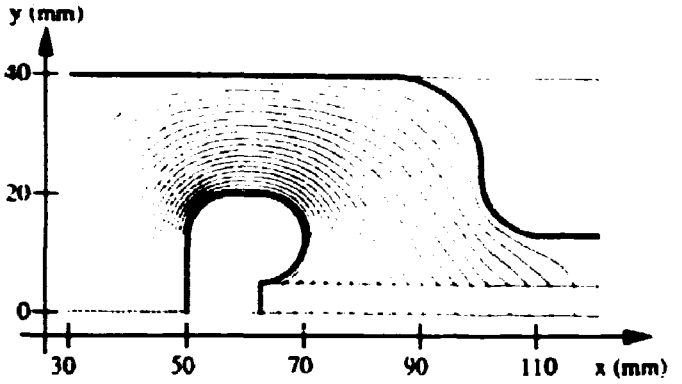

Figure 4 - Poisson plot of equipotential lines for the design of the support insulator between anode and cathode.

5. Prototype Test Results

A 15 cm long prototype of the wire septum has been built to test its high voltage performance in vacuum. Regarding the required wire spacing of 0.65 mm, no signs of breakdown or excessive field emission between the wire plane and the anode have been observed up to anode voltages of 120 kV. Leaving spring wires out does not change the performance.

Without processing, the final insulator design is adjustable up to an anode voltage of 120 kV. An anode voltage of 100 kV has been maintained for more than 100 hours.

6. Septum Construction Design

The attractive force between septum wires and anode is less at the entrance and exit of the septum, due to the field clamps. To achieve a same bending for all wires, in order to minimize the effective septum thickness, the wire stretching force is adjusted for the first and last wires by making the carrier circumference less than half a circle and thus increasing the length of the parallel ends of the spring wires. Regarding the maximum expected beam power, this approach has been optimized for an anode voltage of 56 kV.

The positioning of the wire plane with respect to the beam is achieved by a horizontal support table for the whole septum tank, involving separate systems for a translation and rotation in the range of ±12.5 mm and ±0.5° in steps of 0.1 mm and 0.1 mrad respectively.

The whole tank is 1200 mm long, 400 mm wide and 300 mm high. The carrier and anode construction is supported from the top flange. Opposed to the wire plane an open piece of beampipe surrounds the circulating beam, as shown in Figure 5, in order to avoid that the tank will act as a cavity in storage mode operation. Because of the expected radiation levels due to beam losses, aluminum has been used as construction material as far as possible.

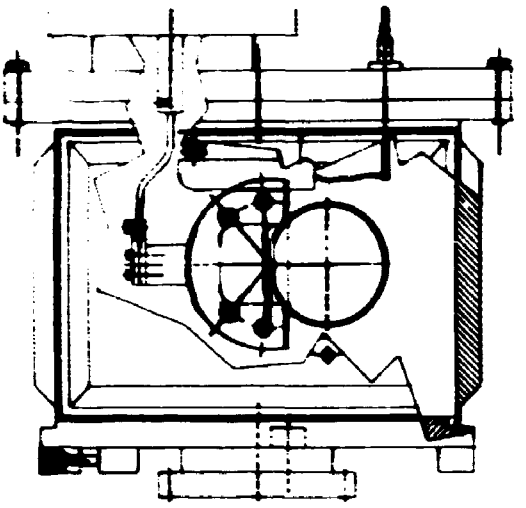

Figure 5 - Assembly drawing of the electrostatic wire septum.

7. Project Status

The construction of the electrostatic extraction septum is finished recently. Installation of the wire septum will follow after the system tests, in order to be in operation during the commissioning of the AmPS ring before the summer of 1992.

8. Acknowledgements

The AmPS project is made possible by financial support of the foundation for Fundamental Research on Matter (FOM).

The authors would like to thank Marco Barens and Marco Kraan (Hogeschool Utrecht) for the contribution in the septum positioning table design. The workshops of NIKHEF are regarded highly for the applied expertise in constructing the septum. The vacuum experts from NIKHEF-K must be thanked strongly for their support in the prototype test set-up.

8. References

[1] G.Luijckx et.al., "The Amsterdam Pulse Stretcher Project (AmPS)", Proceedings 1989 IEEE Particle Accelerator Conference, 1989, Chicago, IL, pp. 46-48.

[2] A.v.d.Linden et.al., "High Power Density, Thin Magnetic D.C. Septa for AmPS", this conference.

[3] R.Maas, "Injection Parameters and Beam Oscillations during extraction", report NIKHEF-K/AmPS/89-07, August 1989.

[4] R.Hoekstra, "Beam Optics of the AmPS Extraction Line", report NIKHEF-K/AmPS/91-01, January 1991.

[5] F.Koechlin, "Un Séparateur Electrostatique pour l'Extraction du Faisceau d'un Anneau d'Electrons", DPh-N/Saclay n.°2378, October 1986.

[6] R.Dubois, N.Garrel, "Tension Positive sur le Septum Electrostatique", report CERN/SPS/Note Techn./78-4, April 1978.

[7] J.H.L.Jonker, "The Internal Resistance of a Pentode", and P.H.J.A.Kleijnen, "The Penetration Factor and the Potential Field of a Planar Triode", Philips Research Reports, Vol. 6, Nr. 1, February 1951.

[8] A.Durand et.al.,"Champ de Fuite des Septums Electrostatiques à Fils", Nuclear Instruments and Methods 165(1979)361-370

[9] D.Anderson et.al., "Particle Detectors", Physics Letters B, Volume 204, 1988, p. 63.

Pulsed Electrostatic Kickers with Low Beam Impedance for AmPS

E. HEINE, A. van der LINDEN, J.H.M. BIJLEVELD, P.J.T. BRUINSMA, J.J. KUIJT, P.F. TIMMER
National Institute for Nuclear and High Energy Physics (NIKHEF),
P.O. Box 41882, 1009 DB Amsterdam, the Netherlands

Abstract

During 3-turn injection into AmPS, the Amsterdam Pulse Stretcher ring, two identical electrostatic kickers create a local vertical displacement of the closed orbit of the ring by a 2.75 mrad bend. Within 10 μs, the 1570 mm long parallel plates of the kickers are charged to + and -35 kV by a triode switch. The fast discharge of the plates, required at the end of the injection cycle of 2.1 μs, is achieved by using very fast thyratrons. A discharge time of less than 100 ns is shown in bench tests.

The synchronous discharge of the two kickers requires a timing error of less than 1 ns. Timing jitter is reduced by the improved stability of the thyratron adjustments.

The measured longitudinal broadband impedance $|Z/n|$ of the kicker is $(0.21 \pm 0.05)\ \Omega$.

1. INTRODUCTION

The AmPS ring aims at a 100% duty cycle operation by means of a slow extraction of injected electron beam pulses of 2.1 μs, as described by Luijckx et.al. [1]. The maximum beam energy is 900 MeV and the maximum current is 80 mA. Used as a storage ring, the maximum beam energy will be 1 GeV.

The two injection kickers in the ring have a symmetrical location with respect to the injection septum magnet [2], as is illustrated in Figure 1. The septum injects beam "off-axis" but parallel to the ring-axis. The first kicker (K1), downstream of the septum, bends the injected beam downward into the horizontal plane of the ring. Upstream of the septum, the second kicker (K2) bends the returning beam downwards to bring it "off-axis" again. Due to the horizontal betatron oscillation of the beam, characterized by a 120° phase shift per turn of the beam position, the injected beam passes the septum from aside at its first and second return. The first kicker directs both the injected and the returning beam back into the horizontal plane.

This scheme allows a 3-turn injection process for AmPS. Just before the third return of the injected beam the two kickers are switched off to avoid beam to hit the septum. The 3-turn injection efficiency is determined by the kicker falltime.

2. KICKER DESIGN REQUIREMENTS

2.1 *Optical requirements*

Maas [3,4] optimized the optics of the injection process. This resulted in a vertical bending angle of 2.75 mrad for both kickers. The total length of the kicker construction, located in between two ring quadrupoles, is restricted to 2120 mm. For ring operation, the beam stay clear requirements are 40 mm in the vertical direction and 80 mm in the horizontal direction.

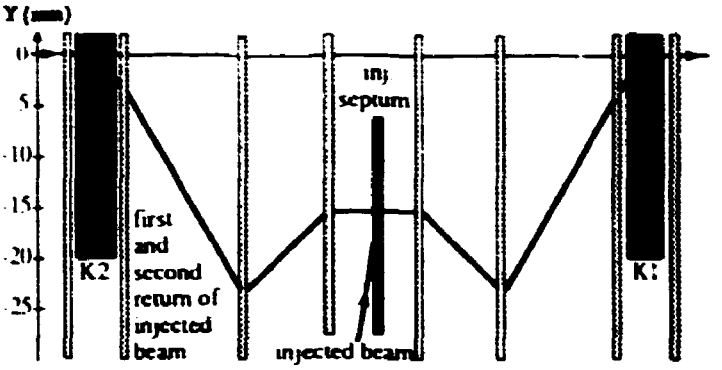

Figure 1 - Schematic layout of the AmPS 3-turn injection process using the kickers (K1,K2) and the injection septum.

In the multiturn injection process, the second kicker must be discharged 77.5 ns earlier than the first kicker. During the discharge, as characterized by the falltime, beam arriving at the kicker will be missteered in the vertical plane. To minimize an increase of the vertical emittance the two kickers must be discharged synchronously. The timing accuracy must be about 1% of the falltime, assuming a linear discharge.

In stretcher mode the time for slow extraction is at least 2.5 ms. The required maximum repetition rate for the kicker operation is 400 Hz.

Storage mode operation is sensitive for bunch lengthening effects. The longitudinal broadband impedance $|Z/n|$ of the kickers is required to be less than 1 Ω per kicker.

2.2. *Pulse requirements*

The 3-turn injection process requires the flattop length of the kicker pulse to be 2.1 μs. The risetime of the kicker pulse is allowed to be of the order of 10 μs. This is less than 1% of the minimum time for extraction.

To achieve almost complete 3-turn injection the falltime is required to be less than 10% of one turn revolution time. This restricts the falltime to 70 ns. The relative timing accuracy for the two kickers should be less than 1 ns.

2.3. *Design principles*

Both optical and pulse requirements are regarded to be more suitable for electrostatic than for magnetic kickers. Firstly, the required bending strength is small enough to be realized by an electrostatic deflection. Secondly, for a vertical bending of the kickers, the required large horizontal clearance allows the gap height for electrostatic deflection to be two times smaller than for magnetic deflection. Finally, because the risetime requirement is not critical, the AmPS kicker design can concentrate on the flattop and fast discharge of an electrostatic kicker.

Therefore, the principle design of the AmPS kicker is a parallel plate construction, in analogy to the kicker design of Figley [5]. Considering the pulse requirements, the plates are capacitively charged by a current source, the injected beam is deflected by an electrostatic field and the plates are discharged like a transmission line.

3. KICKER CONSTRUCTION DESIGN

3.1. Design parameters

The combined fast switching of high currents and hold-off of high voltages to charge and discharge the kicker plates requires the use of electron tubes. To ensure a long life time of the tubes, the maximum lower and upper plate voltage is restricted to +35 kV and -35 kV respectively. This enables the use of the EEV B1510 triode as the charging switch and the EEV CX1154D thyratron as the discharging switch.

With regard to the vertical beam stay clear requirements the gap distance between the plates is determined as 40 mm. The maximum electric field strength is then 17.5 kV/cm. To create a bending angle of 2.75 mrad for the maximum beam energy of 1 GeV, the plate length is required to be 1570 mm. This is less than the limit of 2120 mm. For an ideal transmission line discharge the calculated minimum falltime is 10.5 ns.

3.2. Mechanical construction

For reasons of mechanical rigidity, the parallel plate kicker construction consists of standard U-profile aluminum beams of 150 mm width, 50 mm height and 10 mm thickness. The two plates are connected by ceramic bridges to withstand 70 kV. Stand-offs for 25 kV d.c. are used in the hanging construction between the upper plate and the kicker tank of Ø 253 mm, as shown in Figure 2. To minimize contributions to the $|Z/n|$, the change in beam pipe diameter from Ø 90 mm to Ø 253 mm is made by conical tapers. The taper angle is 20°.

The electrical feedthroughs for the two plates are located aside of the kicker tank to create a short electrical length.

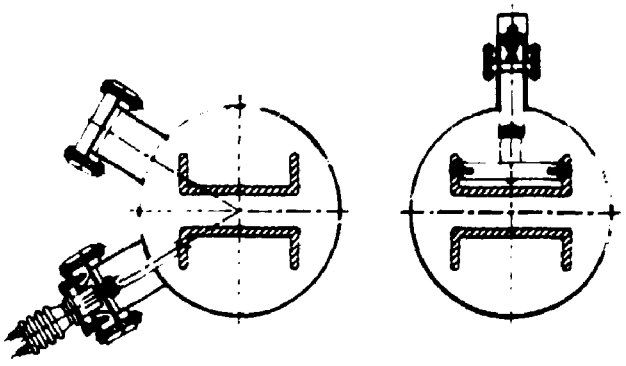

Figure 2 - Cross-sections of the mechanical kicker design.

Having determined the cross-section of the construction, the transmission line impedance of the kicker plates has been simulated using printed circuit board with a resistive layer. Assuming the horizontal symmetry plane is at ground potential, the line impedance of a kicker plate is about 20 Ω.

4. PULSED POWER SUPPLY DESIGN

4.1. System design and mechanical construction

The power supply design is schematically shown in Figur 3. A positive and negative d.c. supply continuously charg separate 250 nF capacitors, which are housed in an oil tank to gether with the electron tubes and the local timing boards an the control voltage supplies. Oil is used for cooling and in sulation, in order to allow a compact construction, with shor electrical lengths for fast switching, and to reduce electromag netic interference. If possible, the use of semiconductors in th tank is avoided to minimize failures due to radiation damage.

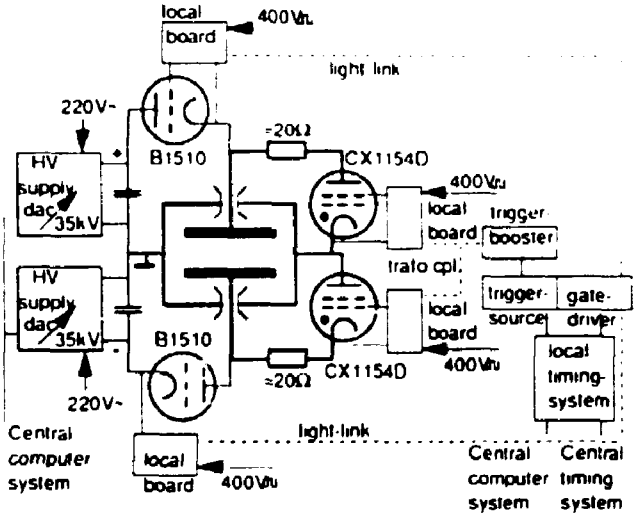

Figure 3 - Schematic layout of the kicker pulsed power suppl

4.2. Charging circuit

The kicker plates are capacitively charged from the 250 nl capacitors using the light-link controlled EEV B1510 triode a high current, high voltage switch. The triode filament voltag is adjustable to operate the circuit as a constant current sourc of 1 A at maximum voltage. The required performance is wel below the maximum ratings [6], while the minimum chargin time is less than 10 µs. Cooling of this glass type electro tube is strongly recommended.

4.3. Discharging circuit

The EEV deuterium filled ceramic thyratron CX1154D chosen as very fast high current, high voltage discharge switc because, being a one gap-thyratron, it is characterized by very high rates of rise of current of more than 120 kA/µs. As suming an ideal transmission line discharge of a kicker plate the maximum voltage of 35 kV, the peak current is 875 A an the average current is 3.67 mA, which is well below the max mum ratings [7].

The reservoir heating voltage is adjustable in order to find compromise with respect to voltage hold-off and rate of rise current as well as for reasons of thyratron life time. The hig power trigger pulse is delivered by a small CX1548 thyratro used as booster, and amplified by a trigger transformer. T maximize the trigger pulse energy, the grid circuit involves differentiator without coupling between control and bias gri

Jitter in triggering is reduced by the d... filament voltage supply in order to avoid electromagnetic fields at the cathode.

An optimal transmission line discharge of the kicker plates is achieved by tuning the matched load in the discharge circuits during the final development of the power supply system.

4.4. *Timing*

The charging of the kickers is timed by the delayed pulse generator (dpg) of the linac beam switch yard. The timing of the discharge makes use of the dpg of the ring timing system. Finally, the timing of the relative discharge of the two kickers is adjustable within the integrated kicker control system with the aim of reducing relative timing errors.

4.5. *Test results*

The charging and discharging of one kicker plate, with the other plate at ground potential, has been tested up to 20 kV in air, including a test of the prototype timing system. As shown in Figure 4 a fast falltime of less than 100 ns, similar to the discharge of a transmission line, has been achieved.

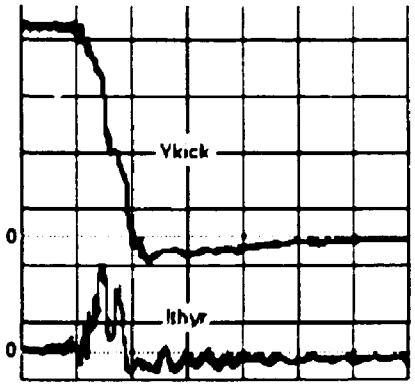

Figure 4 - Measured kicker plate discharge in bench test. Scale is 5 kV/div, 106 A/div and 50 ns/div respectively.

5. KICKER BROADBAND IMPEDANCE

The longitudinal coupling impedance Z of the kicker, with respect to the standard ring beampipe, is determined in coaxial wire measurements, involving a small centred conductor, that simulates the beam position in storage mode. A 20 GHz HP network analyzer is used to send calibrated signals along the centred conductor and to measure the signal transmission. According to Hahn and Pedersen [8]:

$$|Z| = 2Z_0 \cdot \left(\frac{S_{21\ \text{beampipe}}}{S_{21\ \text{kicker}}} - 1 \right) \qquad (1)$$

S_{21} is the measured transmission in S-parameters; Z_0 is the transmission line impedance of beampipe and centre conductor.

The frequency spectrum of Z is used to determine an upper limit of the parasitic mode loss factor K:

$$K(\sigma, f_0) < 2f_0 \cdot \sum_{n=1,2,\ldots} |Z(n f_0)| \cdot e^{-(n 2\pi f_0 \sigma)^2} \qquad (2)$$

where σ is the bunch length and f_0 is the revolution frequency.

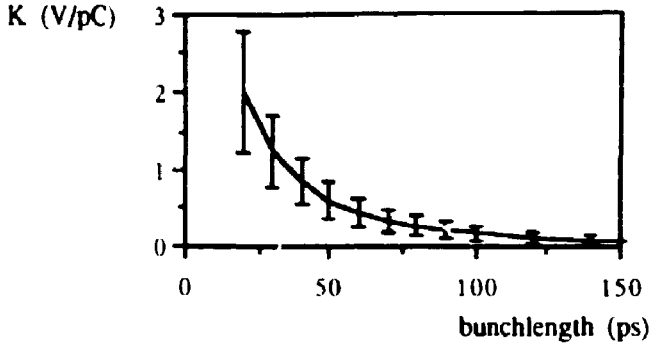

Figure 5 - Parasitic mode loss factor K of a kicker, calculated as a function of the bunchlength.

As shown in Figure 5, K is calculated for the revolution frequency of 1.41666 MHz and for bunch lengths of 20 ps and higher. The data are fitted with a broadband resonator model by Maas [9]. As result for the $|Z/n|$, the longitudinal broadband impedance of the kicker is calculated as $(0.21 \pm 0.05)\ \Omega$.

6. PROJECT STATUS

Both kicker tanks have already been installed in the ring. The construction and system test of the power supply tank is in its finishing stage. Before the summer of 1992 the first kicker will be used for single turn injection into AmPS.

7. ACKNOWLEDGEMENTS

The AmPS project is made possible by financial support of the foundation for Fundamental Research on Matter (FOM).

The authors would like to thank Dr.F. Caspers (CERN) for advices on coaxial wire measurements. F. Kroes, J. Noomen and T. Sluijk (NIKHEF) are thanked for the introduction in rf techniques. The students F. Hermsen, P. Ouwerschuur, H. Jagers (r.k. TH Rijswijk) and M. Anthonijsz (HTS Amsterdam) are regarded highly for performing network analyzer measurements and for the development of software, necessary for loss factor calculations. Finally, R.Pirovano (NIKHEF) has largely contributed to the development of the kicker timing system.

8. REFERENCES

[1] G.Luijckx et.al., "The Amsterdam Pulse Stretcher Project (AmPS)", Proceedings 1989 IEEE Particle Accelerator Conference, 1989, Chicago, IL, pp. 46-48.

[2] A.v.d.Linden et.al., "High Power Density, Thin Magnetic D.C. Septa for AmPS", this conference.

[3] R.Maas, "Injection Parameters and Beam Oscillations during extraction", report NIKHEF-K/AmPS/89-07, August 1989.

[4] R.Maas, "Timing Injectiekickers", internal note, Jan. 1991.

[5] C.B.Figley, "A High Speed Electrostatic Kicker for the Pulse Stretcher Ring at SAL", Nuclear Instruments and Methods in Physics Research A273 (1988) 59-62.

[6] Datasheet EEV B1510 high voltage control triode, July 1977

[7] Datasheet EEV CX1154D CX1154E Deuterium Filled Ceramic Thyratrons, December 1986.

[8] H.Hahn, F.Pedersen, "On Coaxial Wire Measurements of the Longitudinal Coupling Impedance", BNL 50870, April 1978.

[9] R.Maas, private communication.

High Power Density, Thin Magnetic D.C. Septa for AmPS

A. van der LINDEN, J.H.M. BIJLEVELD, H. BOER ROOKHUIZEN, P.J.T. BRUINSMA, M. DOETS, P. LASSING, C. ZEGERS
National Institute for Nuclear and High Energy Physics (NIKHEF),
P.O. Box 41882, 1009 DB Amsterdam, the Netherlands

Abstract

Both the injection and extraction line of the Amsterdam Pulse Stretcher ring (AmPS) contain a d.c. septum magnet.

The 400 mm long injection septum, located inside the ring vacuum, requires 1075 A in its winding to generate the maximum field of 0.135 T. The septum thickness at the exit is restricted to 3 mm. The septum is cooled indirectly by using ceramic enamel of 0.2 mm thickness for electrical insulation. Tests at 1 kA in vacuum show a 80 °C temperature rise of the winding due to the 300 W dissipation. The heat conductivity of ceramic enamel is at least 0.2 W/m.°C. The stray field is measured to be at maximum 8 Gauss at 850 A.

The 700 mm long extraction septum is outside the vacuum and consists of 2 turns to generate a maximum field of 0.271 T at 2160 A. The septum thickness is 5 mm at the entrance. Water cooling is required for the maximum dissipation of 2 kW/m. The mean temperature rise of the windings is measured to be 2.5 °C at 1060 A. The maximum integrated stray field at 750 A is measured to be 0.3 mT.m.

1. INTRODUCTION

The AmPS ring aims at a 100% duty cycle operation by means of a slow extraction of injected electron beam pulses of 2.1 μs, as described by Luijckx et.al. [1]. The maximum beam energy is 900 MeV and the maximum beam current is 80 mA.

The injection septum directs the beam parallel to the ring axis by a downward bend. In the 3-turn injection process a set of two injection kickers [2] brings the injected beam on-axis vertically. The septum magnet is located in the ring vacuum because of the close passage of circulating beam. The required bending strength is related to storage mode operation with a maximum beam energy of 1 GeV.

The magnetic extraction septum bends the extracted beam, initially intercepted and separated from the circulating beam by the electrostatic extraction septum [3], away from the ring in the horizontal plane. The initial beam separation has been enlarged sufficiently by two ring quadrupole magnets to locate the magnet outside the ring vacuum.

2. THE MAGNETIC INJECTION SEPTUM

2.1. *Optical requirements*

Stretcher ring operation requires the injection of beam in hollow horizontal phase space. This enables 3-turn injection. As shown in Figure 1, in real space the injected beam passes the injection septum from aside after one and two turns.

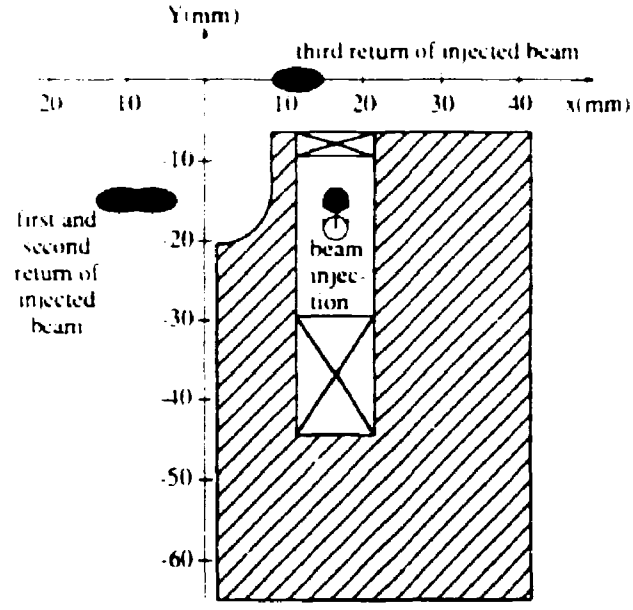

Figure 1 - The 3-turn injection process, as seen from the exit of the injection septum.

Because the injection kickers have been switched off fastly, the beam circulates in the horizontal plane after 3 turns.

Maas [4] has optimized the ring lattice with respect to both the injection process and the kicker design. As a result, shown in Figure 1, the septum thickness at the exit as well as the thickness of one yoke leg is restricted to 3 mm. The length of the injection septum is limited to 400 mm, because of the ring beam stay clear requirements.

The design of the injection line by Van der Laan [5] has resulted in a bending radius of the magnetic injection septum of 25 m. The total bending angle is 16.2 mrad. The maximum required magnetic induction in the gap is 0.135 T. To allow safe beam transport through the magnet, the gap height has been determined to be 10 mm, as indicated in Figure 1.

2.2. *Electrical requirements and power dissipation*

For reasons of electrical insulation and stray fields, the injection septum consists of one winding. The required maximum excitation current is 1075 A. The conductor thickness is increased from exit to entrance by a 25 m bending radius. The maximum power dissipation is 500 W/m for the total, cold septum conductor and even 650 W/m at the exit.

D.c. excitation of a solid steel magnetic injection septum is given preference with respect to pulsed excitation of ferrite or laminated cores, because of vacuum requirements. Both the cooling of the dissipated power and the generated stray fields, experienced by the circulating beam, have been investigated.

2.3. Cooling requirements and heating tests

Because of the small dimensions of the septum conductor, an indirect cooling technique has been developed by regarding thermal conduction of heat to the water cooled magnet yoke. Therefore, the cooling requirements are strongly related to the thermal properties of the electrical insulation between septum conductor and yoke. The coefficient of heat transfer, defined as the ratio of the heat conductivity of the insulation material and its thickness, has to be maximized.

The use of ceramic enamel for electrical insulation, as suggested by Bijleveld et.al. [6], has been investigated. By means of an industrial baking process, FERRO Holland B.V. [7] has provided pieces of magnet steel with 0.25 mm thick layers of ceramic enamel. By machining, the layer thickness is reduced to 0.2 mm.

The final construction of the magnetic injection septum is tested up to 1000 A, in vacuum. The total power dissipation is determined by measuring the winding resistance, being 0.32 mΩ at the cooling water temperature of 35 °C. Assuming in worst case that the increase in resistance is due to the increase of the septum conductor resistance, the mean temperature rise of the copper septum conductor is estimated. The test results are shown in Figure 2. By extrapolation, the mean temperature rise at 1075 A is 105 °C and the maximum temperature rise at the exit is 140 °C. The heat transfer coefficient for the ceramic enamel insulation layer is at least 1000 W/m^2.°C; the thermal conductivity of the ceramic enamel is at least 0.2 W/m.°C.

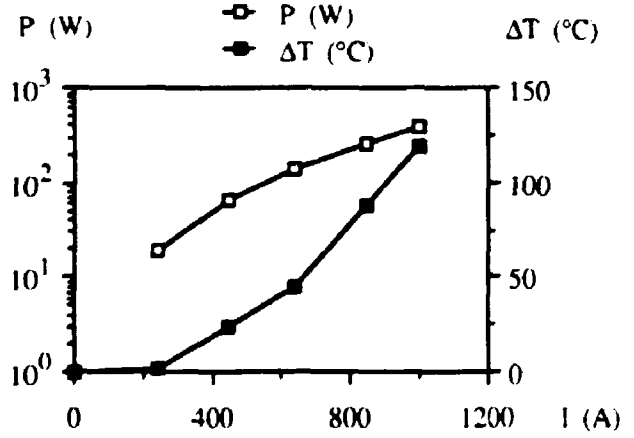

Figure 2 - The measured power dissipation P and maximum temperature rise ΔT as a function of the current I in the test of the final injection septum construction.

2.4. Stray field calculations and measurements

The stray field of the final construction of the magnetic injection septum is measured at 850 A in a computer controlled Hall probe measurement set-up. In the horizontal plane of the ring only the vertical field component is measured, because of the finite dimensions of the probe. The maximum measured value is 8 Gauss at 850 A.

The integrated vertical field in this plane varies from -0.15 mT.m to +0.15 mT.m, as shown in Figure 3. At 3 mm above the horizontal plane of the ring both field components have been measured. The resulting maximum integrated horizontal field is 0.2 mT.m, also shown in Figure 3.

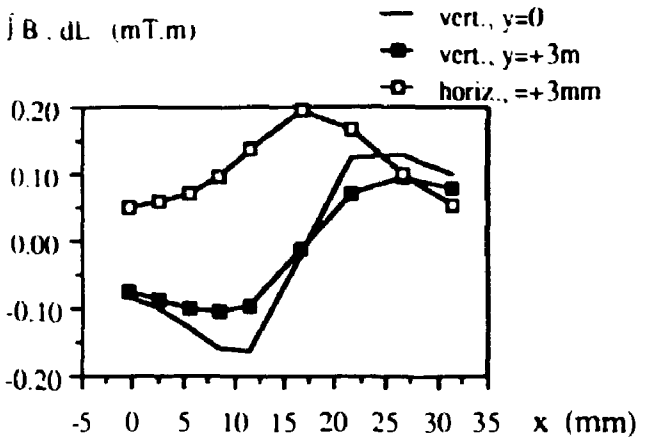

Figure 3 - The integrated stray field of the injection septum, related to the ring coordinate system, measured at 850 A.

Considering the bending strength of steering magnets in the ring, being 3.3 mT.m for both the horizontal and vertical direction, the measured stray fields are regarded small enough for controlled ring operation.

2.5. Septum construction design

The septum magnet construction includes a gildplated coil and a nickelplated yoke to prevent oxidation. Cooling tubes are brazed into the two yoke parts, that are bolted together.

Tapers provide a smooth transition from the standard beampipe of 90 mm diameter to the septum tank of 119 mm diameter. Being a perturbation for the beam during ring operation in storage mode, the septum magnet is screened by wedge-shaped copper blocks in front of and at the back of the magnet construction.

2.6. Project status and operation performance.

At the end of 1990 the magnetic injection septum has been installed in the AmPS injection line. In the spring of 1991 it has been taken into operation. During injection line tests, the first successful performance has been achieved in the autumn of 1991 with 3 μs long beam pulses with an energy of 150 MeV and a current of 3 mA, at a repetition rate of 10 Hz.

3. THE MAGNETIC EXTRACTION SEPTUM

3.1. Optical requirements

The separation between the extracted and circulating beam is optimized in relation to the bending strength and horizontal position of the electrostatic extraction septum. This enables a fixed location of the magnetic extraction septum, outside of the vacuum, downstream of the second ring quadrupole magnet, downstream of the electrostatic extraction septum.

At minimum, shown in Figure 4, the horizontal separation is 22 mm. Having 5 mm space for the extracted beam, 10 mm for the circulating beam and 1 mm thick beampipe walls, the septum thickness at the entrance is restricted to 5 mm.

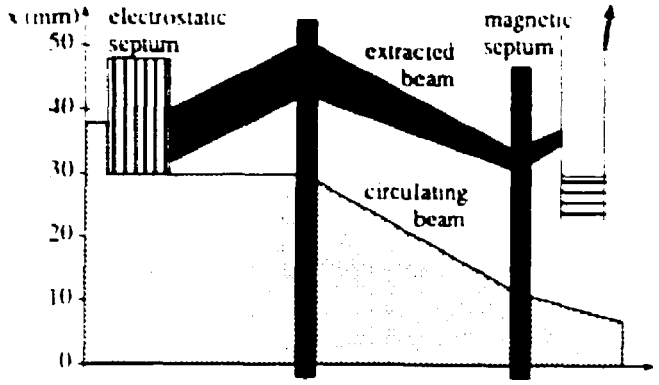

Figure 4 - Schematic layout of beam extraction, optimized in relation to the maximum excursions of the circulating beam.

The extracted beam is bent parallel to the ring axis by the first two extraction line magnets, as described by Hoekstra [8]. This requires the horizontal position of the extracted beam to be 220 mm at the entrance of the first of these magnets, 3 m behind the septum magnet entrance. The bending angle of the septum magnet is optimized as 63.3 mrad for a length of 700 mm. The bending radius of 11.1 m requires a maximum field strength of 0.271 T for a beam energy of 900 MeV. Regarding the vertical emittance of the extracted beam, the gap height is required to be 20 mm.

3.2. Mechanical and electrical requirements

Having no vacuum requirements, the septum magnet has a two turn coil. The windings are directly water cooled in parallel. The required maximum d.c. excitation current is 2160 A. The septum winding thickness along the magnet is increased by a bending radius of 11.1 m. A square copper conductor with an internal cooling channel of 3 mm diameter is used to construct the windings. Kapton sheet of 0.07 mm is used for electrical insulation. This material has a high radiation resistance. In Figure 5, the assembly of magnet and beampipes is shown.

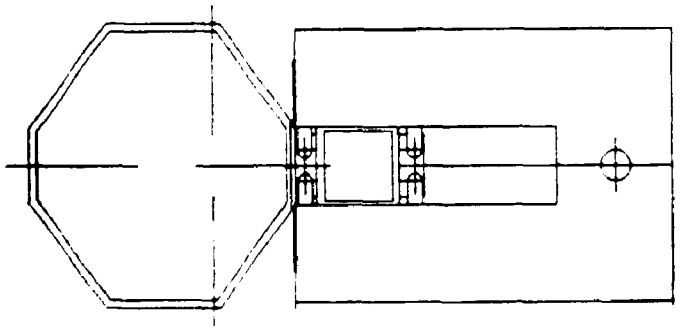

Figure 5 - Assembly drawing of the magnetic extraction septum and the beampipes of the ring and the extraction line.

The current transfer cable consists of copper strips with a total cross section of 2000 mm^2, cooled in the air. The power dissipation is calculated as 40 W/m at maximum current.

3.3. Power dissipation and cooling requirements

The maximum power dissipation in the windings, having minimum dimensions of 5 mm width and 10 mm height, is 2 kW/m at maximum current. A turbulent water flow of 0.5 litre/minute is required to limit the temperature rise of the conductors to 25 °C. The required water pressure is 1 bar.

3.4. Heating tests and stray field measurements

The final construction of the magnetic extraction septum has been tested up to 1060 A. From the increase of the coil resistance, being 0.47 mΩ at the cooling water temperature of 35 °C, the mean temperature rise of the copper coil is 2.5 °C. The maximum temperature rise at the septum entrance is estimated as 8 °C. By extrapolation, at 2160 A the temperature rise is 33 °C at the septum entrance. Because parallel cooling has not yet been applied, the results agree with the design.

At 750 A the stray field of the magnetic extraction septum has been measured. The integrated field, experienced by the circulating beam, is at maximum 0.15 mT.m in the horizontal direction and 0.3 mT.m in the vertical direction. By linear extrapolation, the integrated field at maximum current is found small enough to correct the beam by the steering magnets.

3.5. Status

The magnetic extraction septum has been recently installed at the junction of ring and extraction line. Before the summer of 1992 the first beam will be extracted from the ring for nuclear physics experiments.

4. ACKNOWLEDGEMENTS

The AmPS project is made possible by financial support of the foundation for Fundamental Research on Matter (FOM).

The authors would like to thank FERRO Holland B.V. for providing the injection septum with ceramic enamel. J. Kuijt (NIKHEF) and R. Leenheer are thanked for the support of the magnetic measurements. M. Zoer (NIKHEF) is highly regarded for the construction of the magnetic extraction septum.

5. REFERENCES

[1] G.Luijckx et.al., "The Amsterdam Pulse Stretcher Project (AmPS)", Proceedings 1989 IEEE Particle Accelerator Conference, 1989, Chicago, IL, pp. 46-48.

[2] E.Heine et.al., "Pulsed Electrostatic Kickers with Low Beam Impedance for AmPS", this conference.

[3] A.v.d.Linden et.al., "80 kV Electrostatic Wire Septum for AmPS", this conference.

[4] R.Maas, "Injection Parameters and Beam Oscillations during extraction", report NIKHEF-K/AmPS/89-07, August 1989.

[5] J.v.d.Laan, "Proposed Injection Layout", internal note, September 1989.

[6] J.Bijleveld et.al., "DC Septum Magnets for the Damping Rings of the SLAC Linear Collider, SLAC-PUB-4028, July 1986.

[7] FERRO Holland B.V., Rotterdam, the Netherlands.

[8] R.Hoekstra, "Beam Optics of the AmPS Extraction Line", report NIKHEF-K/AmPS/91-01, January 1991.

IMPROVEMENT OF THE 400 KV LINAC ELECTRON SOURCE OF AmPS

F.B. Kroes, M.G. van Beuzekom, N.J. Dobbe, J.T. van Es, P.P.M. Jansweijer, A.H. Kruijer, G. Luigjes, T.G.B. Sluijk
NIKHEF-K
P.O.Box 41882, 1009 DB Amsterdam, The Netherlands

Abstract

The installation of the 900 MeV Amsterdam Pulse Stretcher (AmPS) is nearly completed and its commissioning will start spring 1992. The existing linac MEA will inject electrons in the AmPS ring. The linacs peak current will be increased from 20 to 80 mA. This requires the modification of the 400 kV low emittance gun which now will deliver a peak current of maximum 400 mA instead of 100 mA at a pulse width of 2.1 μsec. The fourfold increase of the peakcurrent is obtained by doubling both the gun perveance (new gun part) and the pulsed extractor voltage. After chopping and pre-bunching more than 80 mA will be available for acceleration in MEA. To obtain optimum beam quality over this increased current range the hot deck electronics, operating at -400 kV, has been exchanged by a state of the art fast high voltage FET switching supply. The increased space charge forces in the beam require stronger electrostatic focussing in the first electrostatic gap to define the beam diameter at the gun exit. This is accomplished with a 25 kV controlled power supply. A build in microprocessor, coupled to the local computer by optical fibers, is used to monitor and control the gun parameters. The 5kV gun extractor voltage pulse shape can be monitored by means of an analog fibre transducer with build in calibration. Finally, in order to improve the energy stability of the accelerated electrons a serial electron-tube stabilizer was added to the 400 kV DC power supply. A supply stability of 2. 10^{-5} has been achieved.

INTRODUCTION

For 3-turn injection in AmPS, MEA should deliver a 2.1μs pulsed beam at 400Hz, with a peak current of 80mA and taking into account a beamloss of 10% an extracted CW beam of 60μA should be available for the physics experiment.[1]
With an RF chopped bunch length of 120° and a corresponding transmitting efficiency through the chopper collimator of 20-24% a peak current of 400mA must be extracted from the 8mm diameter dipenser cathode button. For generation and handling of this fourfold increased beamcurrent an important improvement of the hot deck electronic equipment combined with adaptions in the injector driftspace were necessary.
The increased radial space charge forces of the increased current in this HV injection system gave narrower restrictions to the correct tuning of the chopping parameters. To minimize the contribution of the chopper [2] on the resultant emittance it is possible to match the existing large diameter (7mm) chopping collimator while creating a relatively small waist at the chopper cavity. The beamdiameter at lens1 should be maintained at about 7mm for both high and low peak current operation. To double the microperveance of the gun the distance and shape of the gun's focussing electrodes are changed. The cathode button is still the same. The beam emittance will increase by about a factor of 1.5 for full current operation. The optimum tuning of the injector under high current condition is more critical then for low currents. Much attention is given to the short and longterm stability of the injector behaviour. For this reason all the input voltages delivered by the hot deck electronics and the 400kV ICT are stabilized. For fast diagnostic purpose all the input parameters can be monitored on line. A switchable beamviewer just in front of the chopper collimator gives visible information about the chopping action.

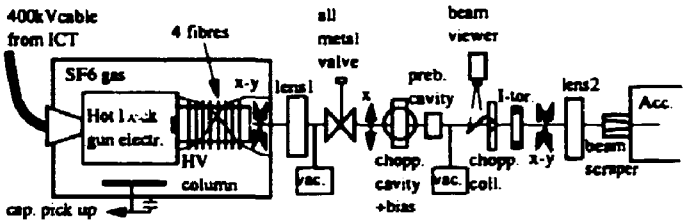

Fig.1 400kV Injector lay out

INJECTOR MODIFICATIONS

Modifications of the injector drift space (fig.1).

- Installation of the high current gun. Microperveance 1.4 in stead of .7 delivered by Haimson Research Corporation.
- Exchange of the O-ring vacuum valve by an all metall type; because of the increased current under space charged limited condition any source to poisson the cathode surface should be avoided.
- Increased strength of lens1 to fulfill the conditon of creating a small waist (1mm) inside the chopper cavity. The chopper cavity with its bias coils is situated halfway between lens1 and the chopper collimator. The strength is increased by insertion of a yoke with smaller diameter.
- Installation of large diameter air bias coils around the TM110 chopper deflection cavity to minimize optical abberations. The former small diameter chopper bias coils were situated just in front of the chopper cavity.
- Installation of a retractable tv screen in front of the chopper collimater for diagnostic information about the chopper.
- Exchange of the cavity type current intensity monitor just behind the chopper collimator by an absolute toroide current monitor, to measure the maximum available peak current for acceleration by MEA and the chopper beam transmission efficiency. Lens2 defines the actual current at the entrance of the accelerator.

Modifications of the electronic hardware (fig.2).

- Variation of the voltage in the first electrostatic acceleration gap to get the correct focussing strength for a certain peak current from the cathode. The voltage between the first

electrostatic acceleration gap defines the strength of this electrical lens and can be changed by adjusting the resistor value. Because optimization of the beam properties for the whole current dynamic range must be possible a remote controlled HV power supply is used for this task.

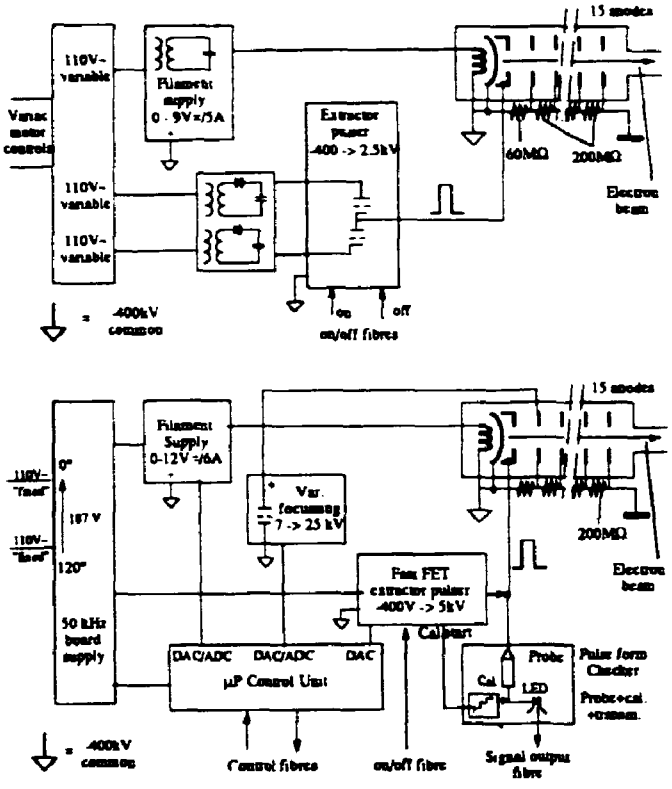

Fig.2 Hot deck gun electronics former (upper) and new (lower) lay out

- Improved extractor switching electronics for a pulse height of 5kV with 50ns rise- and falltime and a stability of 1.10^{-3} which results in a cathode current stability of $1.5\ 10^{-3}$. The fast rise time is requested for better current start definition, which is needed, for beamtransient compensation by the use of spreaded timing of the RF in the 12 accelerator stations of MEA. With the present beam pulse length of 2.1 µs at a peakcurrent of 80mA, the MEA beamloading factor of 2.6MeV/mA and a beamfilltime of 1.25µs, most of the electrons in the beam are subjected to transient beamloading.
- Continuous analog measurement of the extractor pulshape with added calibration signal for accurate level setting; this information is transmitted to earth level by an analog fibre transducer with 10MHz bandwidth.
- µprocessor contol unit at the -400kV level coupled with two fibres for communication with a PC by bitbus protocol; all the gun input parameters are set, read out and watched by this system.
- The former thick fibers are exchanged by new thin (1mm diam.) fibers of which the strength members and coating is removed. The fibers are wrapped around the HV column (1.5turn) making contact with the anodes. Since this modification 5 years ago no fibre was damaged.
- Installation of a capacitive pick up electrode in the 400kV injector tank to measure the ripple and transients (f>10Hz) of the -400kV steady state level.
- Stabilization of the -400kV steady state level to 1.10^{-4} under full load condition. This stabilization is done at the ground level of the -400kV Isolated Core Transformer power supply by means of a tube in series with 4kV of control range.

The modification and extention of the hot deck was so drastic that adaption of the existing hot deck hardware could not be implemented because of the lack of space. Another point of attention was the total weight(23kg) of the hot deck equipment which is mounted at the beginning of the HV column. This hot deck part is hanging on the ceramic HV column. After 15 years of operation a sag of 2mm and several small cracks in the HV column influenced the decision for a total new design with half the weight of the former one.

SOME ELECTRONIC DETAILS

50KHz board supply

The line voltage from the two 110V, 50Hz and 120° phase shifted coupled transformers at the -400kV level in the ICT is transported by wires in the central conductor of the -400kV coaxial cable to the injector vessel. The AC voltage is immediatly converted to DC by rectifying and filtering. This voltage is then chopped by a 50kHz balanced transistor chopper. All the hot deck electronic equipment, such as extractor pulser, filament power, control circuit power and gas circulation fan's are fed by this 50kHz system by means of isolated secundary windings on the central 50kHz supply transformer and by local rectifying, filtering and stabilization circuits. Much attention was given to the adequate screening of this board supply. Smart mechanical constructions were developed to allow fast exchange of parts in case of a faillure

Extractor pulser

The heart of the extractor pulser consists of deck1 to deck8. (Fig.3). The principle is a Marx generator. In rest all the B-switches(FET's) are closed and all the A-switches are opened.

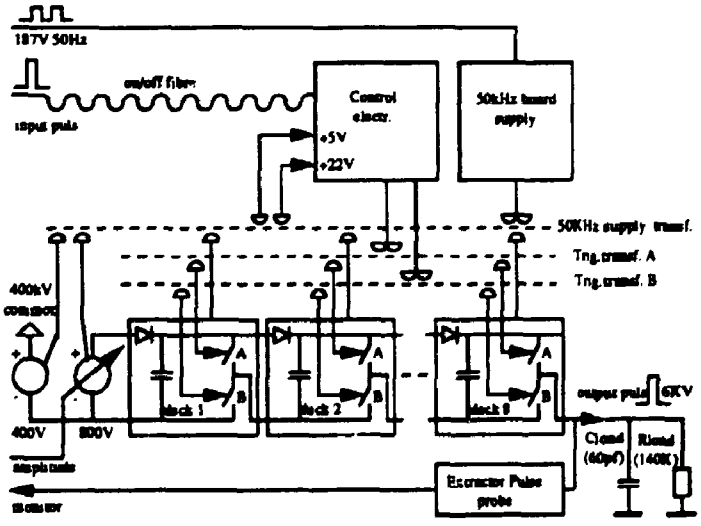

Fig.3 Extractor pulser principle

The rest level of -400V is connected to the output port via all the closed B-switches. The capacitors of decks 1 to 8 are now in parallel connected to the 800V controlled powersupply and are loaded to this level. To create a HV pulse form first of all

the B-switches are opened and after that the A-switches are closed. The diodes prevent the discharge of the capacitors. On the output of the pulser the sum of all the capacitor voltages is delivered. The switches on the decks are controlled by isolated (6kV) trigger transformers A and B. It is important to minimize the parisitic capacity between the decks and the common to optimize the switch speed. The extractor pulse shape will be measured by the already mentioned system.

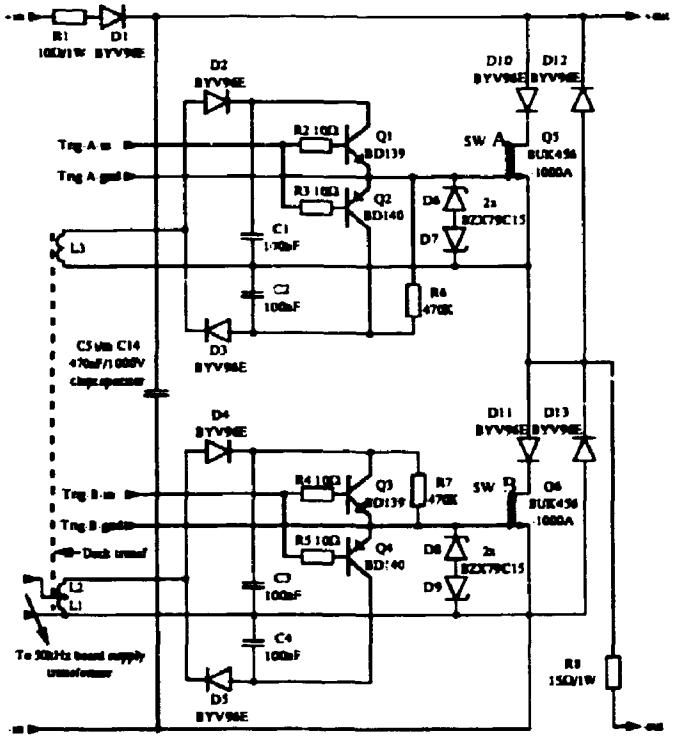

Fig.4 Single deck pulse circuit

In Fig.4 the scheme of one deck module with its components is shown. Switch A and B are driven by push/pull circuits. The primary power is delivered by the 50kHz board supply. The timing and length of the trigger signals for the decks are very crucial.

In Fig. 5 a photopgraph shows the total new design of the hot deck electronics mounted at the beginning of the HV column.

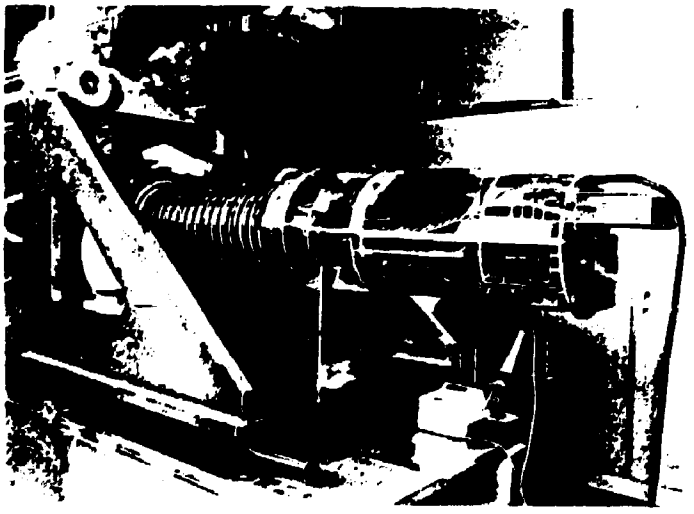

Fig.5 HV Column with hot deck electronics

-400kV stabilization

In the past the -400kV steady state level during the start up of MEA shows changes >1000V caused by respectivily the line voltage stabilizer (400V,10Hz), the stepping transformer control transients (800V,1sec) and the action of the beam safety control device (120V,10Hz). As mentioned earlier the tuning of the injector and MEA with respect to its energy spectrum and corresponding transmission is more critical for high peak currents. The voltage stability should be better then 1.10^{-4}under all beamloading conditions to make this influence negligible. The max. sawtooth ripple at full loaded condition is <100V. Fig. 6 shows the stabilization control scheme.

The series tube only controls the steady state level for frequency changes below 50Hz. The tube control takes care of the stepping transformer control. If the control voltage over the series tube passes a certain lower value the stepping transformer will be activated to increase one step. The reversed action will occur if the control voltage exceeds a certain value. The reference signal is a 16 bits DAC with a stability of 1.10^{-6}. Level control from 0 to -400kV can be done by hand or remote. After installation of this system measurements show a stability of 1.10^{-4} under full range load conditions. The stability is 1.10^{-5} at constant loading.

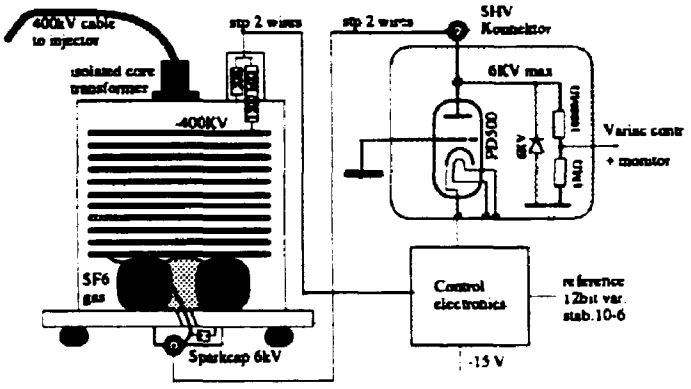

Fig.6 400kV stabilization circuit

ACKNOWLEDGEMENTS

The work described in this paper is part of the research program of the Nuclear Physics section of the National Institute for Nuclear Physics and High Energy Physics(NIKHEF-K), made possible by financial support from the foundation for Fundamental Research on Matter (FOM) and the Netherlands Organization for Scientific Research (NWO)

REFERENCES

[1] G. Luijckx e.a.,"The Amsterdam Pulse Stretcher project (AmPS)", proc.of the IEEE Part.Acc.Conf., Chicago 1989, March 20-23, pp. 46-48

[2] J. Haimson and B. Mecklenburg,"Analysis of high peak current performance of MEA", Haimson Research Corporation. (Proprietary information)

[3] P.P.M. Jansweijer and J.T. van Es,"Extractorpulser", Internal Technical Note, Digel 1990-6

[4] N. Dobbe, T. Sluijk, J.T .van Es, "The ICT 400kV stabilizer", Internal Technical Note, Lino 13,1992